Available online at www.sciencedirect.com

ScienceDirect

Polymer 48 (2007) 5241–5249

polymer

www.elsevier.com/locate/polymer

Synthesis and characterization of novel polyimides derived from 2-amino-5-[4-(4′-aminophenoxy)phenyl]-thiazole with some of dianhydride monomers

Xin Zhao, Yan-Feng Li*, Shu-Jiang Zhang, Yu Shao, Xiao-Long Wang

State Key Laboratory of Applied Organic Chemistry, College of Chemistry and Chemical Engineering,
Institute of Biochemical Engineering and Environmental Technology, Lanzhou University, Lanzhou 730000, China

Received 26 January 2007; received in revised form 8 June 2007; accepted 3 July 2007
Available online 10 July 2007

Abstract

A new kind of aromatic unsymmetrical diamine monomer containing thiazole ring, 2-amino-5-[4-(4′-aminophenoxy)phenyl]-thiazole (APPT), was synthesized. A series of novel polyimides were prepared by polycondensation of APPT with various aromatic dianhydrides *via* one-step process. The resulting polyimides held inherent viscosities of 0.40–0.71 dL/g and were easily dissolved in strong dipolar solvents. Meanwhile, strong and flexible polyimide films were obtained, which had thermal stability with the glass transition temperatures (T_g) of 268.2–328.8 °C in nitrogen, the temperature at 5% weight loss of 452–507 °C in nitrogen and 422–458 °C in air, and the residue at 800 °C of 54.18–63.33% in nitrogen, as well as exhibited outstanding mechanical properties with the tensile strengths of 105.4–125.3 MPa, elongations at breakage of 6–13%. These films also held dielectric constants of 3.01–3.18 (10 MHz) and showed predominantly amorphous revealed by wide-angle X-ray diffraction measurements.

Keywords: Polyimides; Thiazole-containing polyimides; Unsymmetrical ether diamine

1. Introduction

Aromatic polyimides generally possess excellent thermal, mechanical, electrical, and chemical properties. Therefore, they are being used in many applications such as electrics, coatings, composite material, and membranes [1,2]. However, the commercial use of these materials is often limited because of their poor solubility, and high softening or melting temperatures.

To overcome these problems, many efforts have been devoted to enhancing the solubility of polyimides, and this has included the incorporation of flexible linkages [3–5], the introduction of noncoplanar groups [6], or unsymmetrical structure into the polymer backbone [7].

Poly(ether imide)s have attracted great attentions as they may provide good processability owing to the presence of flexible ether links. The development of nucleophilic displacement reactions, and nitrodisplacement reactions in particular, has led to the development of a large class of poly(ether imide)s (PEIs) from various new monomers [8–10]. An important example is Ultem 1000 resin developed and commercialized by General Electric Co., which exhibits reasonable thermal stability and good mechanical properties together with good moldability [11].

Furthermore, the formation of noncoplanar unit through the introduction of heteroaromatic rings with rigid structure into the polyimide backbones keeps the advantages of the rigid rod like polyimides with planar structure, such as interlevel dielectrics and packaging applications including low thermal expansion and excellent mechanical strength [12].

On the other hand, introducing unsymmetrical structure into the main chain of the polyimide can lead to the improvement in

---

* Corresponding author.
E-mail address: liyf@lzu.edu.cn (Y.-F. Li).

0032-3861/$ - see front matter © 2007 Elsevier Ltd. All rights reserved.
doi:10.1016/j.polymer.2007.07.001

solubility and melt processability and other desirable properties [13–19]. Moreover, heteroaromatic rings in the main chain of a synthetic polymer would impart it certain properties expected. The thiazole ring with heteroaromatic structure would have excellent stabilities derived from its molecular symmetry and aromaticity, so new kinds of heteroaromatic monomers holding thiazole unit should have contributions for the chemical stability, thermal and thermooxidative stability. In addition, the thiazole rings in the polyimide backbones which can interact with metal, enhance the adhesion of the polymer chains to metal. However, in our knowledge, there has been very few information concerning polyimides containing thiazole rings until now [20–22].

In this paper, a new kind of thiazole-containing unsymmetrical diamine monomer, 2-amino-5-[4-(4′-aminophenoxy)-phenyl]-thiazole, had been synthesized, successfully. At the same time, a new series of thiazole-containing polyimides were synthesized derived from the resulting diamine monomer, and the polyimides obtained were to be thoroughly characterized. We believe this is a facile synthetic method to modify polyimide. It opens the way to synthesize a series of thiazole-containing unsymmetrical diamines which are easy to be purified.

2. Experimental

2.1. Material

4-Hydroxyacetophenone (TCI) and 4-chloronitrobenzene (TCI) were used as-received. Hydrazine monohydrate (Beijing Chemical reagents Corp., China), bromine (Fuchen Chemical reagents Corp., Tianjin, China), and 5% Pd/C (Acros) were used without further purification. 4,4′-(Hexafluoroisopropylidene)-diphthalic anhydride (6FDA, Aldrich), 4,4′-oxydiphthalic anhydride (ODPA, Shanghai Nanxiang Chemical Co., China), 3,3′,4,4′-benzophenonetetracarboxylic dianhydride (BTDA, Beijing Chemical Reagents Corp., China) were recrystallized from acetic anhydride before use. Pyromellitic dianhydride (PMDA, Beijing Chemical Reagents Corp., China) was purified by sublimation at 200–220 °C. *N*-Methyl-2-pyrrolidone (NMP) and *m*-cresol were distilled under reduced pressure over CaH_2 and P_2O_5, respectively. All other solvents were obtained from various commercial sources and used without further purification.

2.2. Monomer synthesis

2.2.1. 4-(4-Nitrophenoxy)-acetophenone (NPAP)

In a 250-mL three-necked round bottom flask equipped with a nitrogen inlet, 13.62 g (0.1 mol) of 4-hydroxyacetophenone and 29.02 g (0.21 mol) of anhydrous potassium carbonate were suspended in a mixture of 100 mL of dry DMF and 40 mL of toluene. The mixture was then refluxed at 140 °C using a Dean–Stark trap to remove small amount of water azeotropically. After most of the toluene was distilled, 15.76 g (0.1 mol) of *p*-chloronitrobenzene was added when the mixture was cooled to 60 °C. The mixture was then allowed to warm to 120 °C and kept for 6 h. After the reaction mixture was cooled to room temperature, it was poured into 500 mL of ice/water to give brown precipitates. Filtrating and washing with water, the product was recrystallized from ethanol to afford 21.66 g of light yellow crystal NPAP. Yield: 84%. Melting point: 78–79 °C.

^{1}H NMR (200 MHz, $CDCl_3$): δ (ppm) 8.27–8.23 (d, $J = 8.0$ Hz, 2H, H_a), 8.06–8.02 (d, $J = 8.0$ Hz, 2H, H_d), 7.16–7.12 (d, $J = 8.0$ Hz, 2H, H_b), 7.13–7.09 (d, $J = 8.0$ Hz, 2H, H_c), 2.62 (s, 3H, H_e); ^{13}C NMR (200 MHz, $CDCl_3$): δ (ppm) 196.49(C^9), 161.70(C^4), 159.05(C^5), 146.21(C^1), 133.81(C^8), 130.83(C^7), 126.01(C^2), 119.45(C^3), 118.35(C^6), 26.51(C^{10}). Elemental analysis: Calcd. for $C_{14}H_{11}NO_4$ (257.24): C 65.37%, H 4.31%, N 5.44%; found: C 65.32%, H 4.40%, N 5.39%.

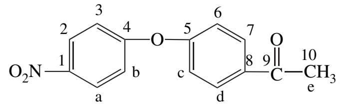

2.2.2. α-Bromo-4-(4-nitrophenoxy)-acetophenone (BNAP)

To a solution of 25.74 g (0.1 mol) of NPAP in chloroform (100 mL), 5.10 mL (0.1 mol) of bromine was added dropwise into the stirred solution at room temperature within 1 h. After complete addition, the mixture was stirred for another 2 h. Excess chloroform was evaporated, and the remaining yellow powder was recrystallized from ethanol to afford 26.22 g of yellow crystal BNAP. Yield: 78%. Melting point: 74–75 °C.

FT-IR (KBr): 1693, 1673 cm^{-1} (α-halogenated ketone), 1511, 1341 cm^{-1} (C–NO_2 stretching), 1341 cm^{-1} (C–N stretching), 1244 cm^{-1} (C–O stretching); ^{1}H NMR (200 MHz, $CDCl_3$): δ (ppm) 8.30–8.26 (d, $J = 8.0$ Hz, 2H, H_a), 8.09–8.05 (d, $J = 8.0$ Hz, 2H, H_d), 7.19–7.15 (d, $J = 8.0$ Hz, 2H, H_b), 7.17–7.13 (d, $J = 8.0$ Hz, 2H, H_c), 4.44 (s, 2H, H_e); ^{13}C NMR (200 MHz, $CDCl_3$): δ (ppm) 189.85(C^9), 161.26(C^4), 159.94(C^5), 143.83(C^1), 130.41(C^8), 126.10(C^7), 119.44(C^2), 118.83(C^3), 118.41(C^6), 30.28(C^{10}); MS(EI): 336 (M^+). Elemental analysis: Calcd. for $C_{14}H_{10}NO_4Br$ (336.14): C, 50.02%; H, 3.00%; N, 4.17%; found: C, 49.96%; H, 2.74%; N, 4.10%.

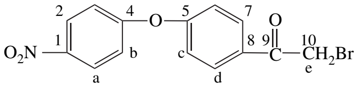

2.2.3. 2-Amino-5-[4-(4′-nitrophenoxy)phenyl]-thiazole (ANPT)

A mixture consisting of 6.72 g (0.02 mol) of BNAP, 1.52 g (0.02 mol) of thiourea and 120 mL of absolute ethanol was put into a reaction flask. The mixture was refluxed for 2 h with stirring before being poured into 400 mL of distiller water and neutralized with ammonia water to form a precipitate. The precipitate was filtrated off, washed with water, recrystallized from ethanol to afford 4.57 g of yellow crystal ANPT, successively. Yield: 73%. Melting point: 174−175 °C.

FT-IR (KBr): 3410 cm^{-1} (NH_2 stretching), 3115 cm^{-1} (associated NH_2 stretching), 1538, 1335 cm^{-1} (C−NO_2 stretching), 1335 cm^{-1} (C−N stretching), 1253 cm^{-1} (C−O stretching); ^{1}H NMR (200 MHz, DMSO-d_6): δ (ppm) 8.27−8.22 (d, $J = 8.6$ Hz, 2H, H_a), 7.91−7.87 (d, $J = 8.6$ Hz, 2H, H_d), 7.19−7.14 (d, $J = 8.6$ Hz, 2H, H_b), 7.17−7.13 (d, $J = 8.6$ Hz, 2H, H_c), 7.02 (s, 1H, H_e); ^{13}C NMR (200 MHz, DMSO-d_6): δ (ppm): 168.24(C^{11}), 162.79(C^4), 153.32(C^5), 148.90(C^1), 142.25(C^{10}), 132.27(C^7), 127.49(C^8), 126.14(C^2), 120.36(C^3), 117.44(C^6), 101.49(C^9); MS (EI): 313 (M^+). Elemental analysis: Calcd. for $C_{15}H_{11}N_3O_3S$ (313.33): C, 57.50%; H, 3.54%; N, 13.41%; found: C, 57.42%; H, 3.49%; N, 13.51%.

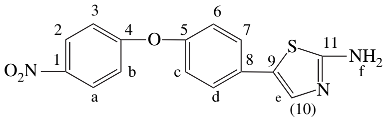

2.2.4. 2-Amino-5-(4-aminophenyl)-thiazole (APPT)

The nitro compound ANPT (15.67 g, 0.05 mol) and 5% Pd/C (0.45 g) were suspended in 150 mL of ethanol in a 250-mL flask. The suspension solution was heated to reflux, and hydrazine monohydrate 80% (20 mL) was added dropwise to the mixture over 0.5 h. After a further 4 h of reflux, the resultant clear, darkened solution was filtered hot to remove Pd/C, and the filtrate was distilled to remove some solvent. The obtained mixture was poured into 200 mL of stirring water, giving rise to pale-yellow product that was isolated by filtration. The crude product was purified by recrystallized from ethanol to afford 12.18 g of yellow crystal APPT. Yield: 86%. Melting point: 180−181 °C.

FT-IR (KBr): 3400, 3322 (NH_2 stretching), 3138 cm^{-1} (associated NH_2 stretching), 1343, 1284 cm^{-1} (C−N stretching), 1238 cm^{-1} (C−O stretching); ^{1}H NMR (400 MHz, DMSO-d_6): δ (ppm) 7.73−7.72 (d, $J = 6.8$ Hz, 2H, H_d), 7.04 (s, 2H, H_f), 6.87 (s, 1H, H_e), 6.85 (s, 2H, H_c), 6.82−6.81 (d, $J = 6.8$ Hz, 2H, H_b), 6.60−6.59 (d, $J = 6.8$ Hz, 2H, H_a), 5.00 (s, 2H, H_g); ^{13}C NMR (400 MHz, DMSO-d_6): δ (ppm) 168.04(C^{11}), 158.16(C^5), 149.43(C^4), 145.42(C^1), 128.93 (C^{10}), 126.86(C^7), 120.87(C^8), 116.24($C^{3,6}$), 114.80(C^2), 99.78(C^9); MS(EI): 283 (M^+). Elemental analysis: Calcd. for $C_{15}H_{13}N_3OS$ (283.35): C, 63.58%; H, 4.62%; N, 14.83%; found: C, 63.50%; H, 4.56%; N, 14.91%.

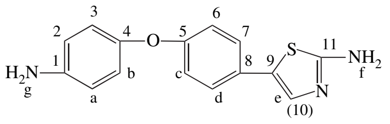

2.3. Polyimide synthesis

The one-step method was applied to polycondensation of objective polyimides. A mixture consisting of 2 mmol of dianhydride, 2 mmol of diamine, and 0.488 g of benzoic acid were added to a 250-mL, three-necked flask which was equipped with a mechanical stirrer, a Dean−Stark trap, a condenser, and a nitrogen inlet/outlet tube. About 12 mL of *m*-cresol was added and then the reaction mixture was heated at 80 °C for 3 h and then at 180 °C for 6 h. Next, 0.52 g of isoquinoline was added to the reaction, and it was heated at 180 °C for another 9 h. The reaction mixture was cooled to room temperature and precipitated into an excess of methanol. The precipitated polyimide was collected by filtration and was dried in a vacuum oven at 120 °C for a period of 6 h and then at 150 °C for 24 h. Yields greater than 96% were obtained.

2.4. Film preparation

The polymers were dissolved in NMP at a concentration of 5−10 wt% and then filtered through sand-bed filter. The filtered solutions were coated on a glass plate and dried in a temperature-controlled oven at 100 °C for 24 h. The prepared films were peeled from the plates and dried in a vacuum at 100 °C for 24 h.

2.5. Measurements

The inherent viscosities of the resulting polyimides were measured with an Ubbelohde viscometer at 30 °C. FT-IR spectra (KBr) were recorded on a Nicolet NEXUS670 Fourier transform infrared spectrometer. ^{1}H NMR and ^{13}C NMR spectra of the diamine and polyimides were measured on a JEOL EX-400 spectrometer using tetramethylsilane as the internal reference. ^{1}H NMR and ^{13}C NMR spectra of the intermediate BNPT and ANPT were measured on a JEOL EX-200 spectrometer using tetramethylsilane as the internal reference. Elemental analyses were determined by a Perkin−Elmer model 2400 CHN analyses. The mechanical properties were measured on an Instron 1122 Tensile Apparatus with 100×5 mm specimens in accordance with GB 1040-79 at a drawing rate of 100 mm/min. The dielectric constant was determined on an Agilent 4291B instrument with 25 μm thinkness specimens at a frequency of 10 MHz at 25 °C. The water uptake values of the films were determined by weighing the changes in vacuum-dried film specimens before and after immersion in deionized water at 25 °C for 3 days. Testing of differential scanning calorimetry (DSC) were performed on a Perkin−Elmer differential scanning calorimeter DSC 7 or Pyris 1 DSC at a scanning rate of 20 °C/min in flowing nitrogen (30 cm^3/min), and glass transition temperatures (T_g) were read at the DSC curves at the same time. Thermogravimetric analysis (TGA) was conducted with a TA Instruments TGA2050, and experiments were carried out on approximately 10 mg of samples in flowing air (flowing rate = 100 cm^3/min) at a heating rate of 20 °C/min. Wide-angle X-ray diffraction measurements were performed at room temperature (about 25 °C) on a Siemens Kristalloflex D5000 X-ray diffractometer, using nickel-filtered Cu Kα, radiation ($\lambda = 1.5418$ Å, operating at 40 kV and 30 mA).

3. Results and discussion

3.1. Composition and structure of diamine monomer (APPT)

Novel diamine monomer, i.e. 2-amino-5-[4-(4′-aminophenoxy)phenyl]-thiazole (APPT) was synthesized by four step procedures, as shown in Scheme 1. Firstly, α-bromo-4-(4-nitrophenoxy)-acetophenone (BNAP) was formed by bromination of 4-(4-nitrophenoxy)-acetophenone (NPAP), which was synthesized by nucleophilic substitution reaction of *p*-hydroxyacetophenone with *p*-chloronitrobenzene. Then nitro compound, 2-amino-5-[4-(4′-nitrophenoxy)phenyl]-thiazole (ANPT), was synthesized by the ring formation of BNAP with thiourea, and ANPT was converted to APPT by reduction of the nitro groups into NH_2 groups by catalytic hydrogenation of them with Pd/C in ethanol. Based on the better solubility of ANPT than traditional symmetrical two nitro compounds, the diamine monomer was easy to be purified. The new aromatic diamine monomer is stable in atmosphere at room temperature.

FT-IR, NMR, and elemental analysis were used to confirm the structures of the intermediate BNAP, ANPT and the diamine monomer (APPT). Fig. 1 shows FT-IR spectra of the diamine monomer (APPT), and its intermediate BNAP, ANPT. The FT-IR spectra of BNAP gave characteristic bands at 1693, 1673 cm^{-1} (α-halogenated ketone). After the ring formation of BNAP, the resulting nitro compound ANPT gave two characteristic bands indicating asymmetric and symmetric stretching of NO_2 group at 1538, 1335 cm^{-1}, especially. The diamine monomer (APPT) obtained by reduction of ANPT illustrates that there are characteristic absorption of the amino group showed a pair N–H stretching bands in the region of 3400–3322 cm^{-1} and a associated N–H stretching band at 3138 cm^{-1}. However, the corresponding absorption bands of the nitro group have disappeared. The FT-IR spectra confirm the reaction mechanism shown by Scheme 1.

Fig. 2 shows the ^1H NMR and ^{13}C NMR spectra of the diamine APPT, in which its chemical structure was clearly identified. As shown in Fig. 2(a), the absorption peaks appeared at 5.0 ppm and 7.0 ppm in the ^1H NMR are assigned to the amino protons of benzene and thiazole ring, which indicated the presence of unsymmetrical structure. All intermediate compounds and the diamine were also confirmed by elemental analysis, which were in good agreement with the calculated values, as reported in Section Experimental. The results indicate that the design and synthesis of novel diamine monomer APPT should be successful and feasible in this work.

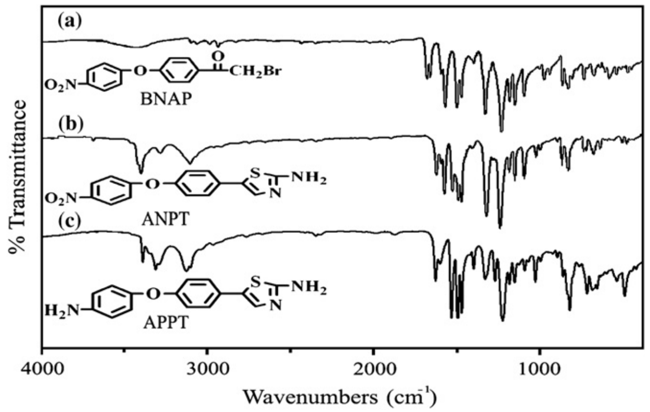

Fig. 1. FT-IR spectra of BNAP (a), ANPT (b) and APPT (c).

3.2. Synthesis chemistry of polyimides

A series of polyimides were prepared from the polycondensations of diamine monomer APPT with various commercially available aromatic tetracarboxylic dianhydrides including 4,4′-(hexafluoroisopropylidene)diphthalic anhydride (6FDA), 4,4′-oxydiphthalic anhydride (ODPA), 3,3′,4,4′-benzophenonetetracarboxylic dianhydride (BTDA), pyromellitic dianhydride (PMDA), *via* one-step synthetic method, as shown in Scheme 2. These polyimides were prepared by high temperature polycondensation reactions in a high boiling solvent (*m*-cresol) at 180–190 °C. The formation of the *trans*-isoimide was promoted by the acidic catalyst, which was added in the first step. Then, the conversion of the *trans*-isoimide to polyimide needed a basic catalyst [23,24]. The inherent viscosity of the polyimides was significantly affected by the nature of the catalysts, mole ratio of the catalysts and dianhydrides, and addition order of the catalysts [25]. The most effective catalyst was benzoic acid (2 mol)

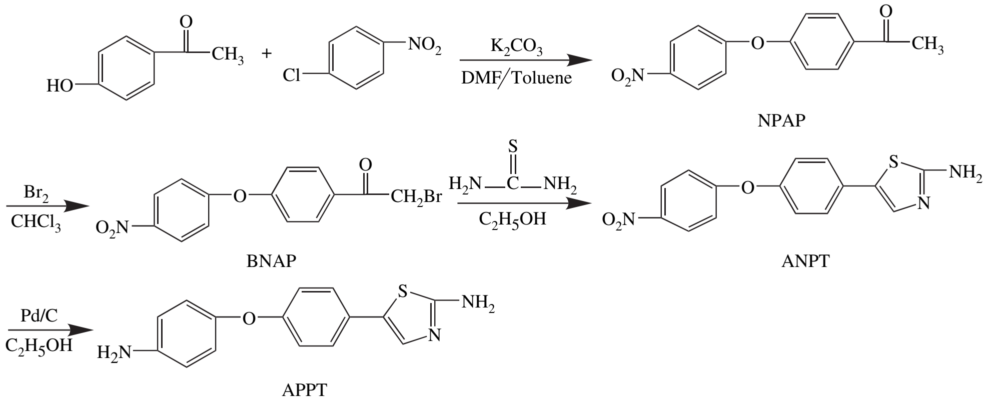

Scheme 1. Synthesis of 2-amino-5-[4-(4′-aminophenoxy)phenyl]-thiazole.

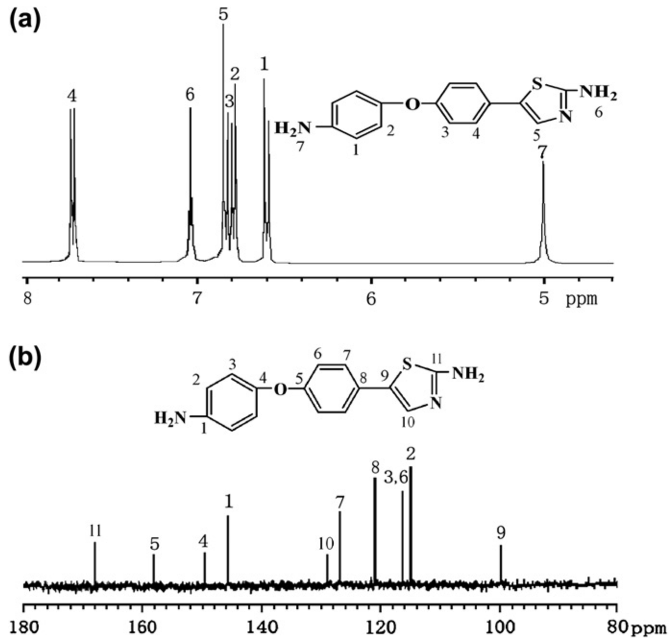

Fig. 2. ^{1}H (a) and ^{13}C (b) NMR spectra of APPT.

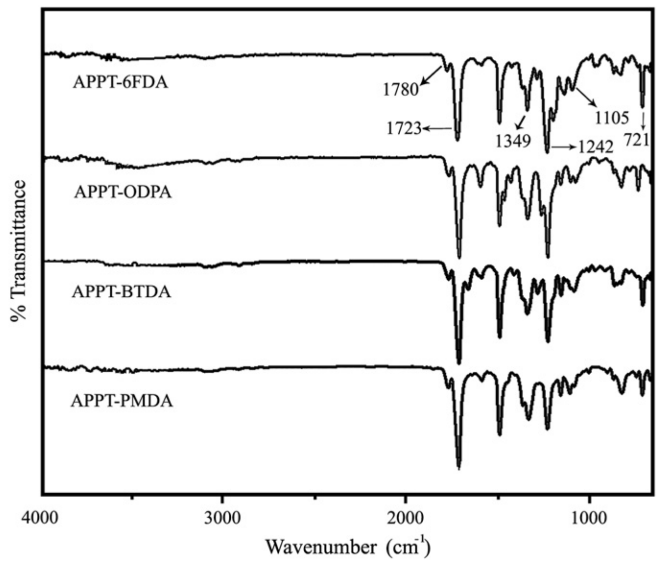

Fig. 3. FT-IR spectra of polyimides.

that with dianhydride (1 mol) added at the beginning of the reaction, and then isoquinoline (2 mol) was added after a few hours. The structural features of the polyimides were identified with FT-IR and ^{1}H NMR. FT-IR spectra of these polyimides are illustrated in Fig. 3. We observed all the expected bands at 1780 and 1723 cm^{-1} (asymmetrical and symmetrical C=O stretching), 1349 cm^{-1} (C–N stretching), 1105 and 721 cm^{-1} (imide ring deformation). In addition, a peak at 1242 cm^{-1} appeared due to the presence of ether linkage in the polymer structure. Fig. 4 shows the high-resolution ^{1}H NMR spectrum of PI derived from APPT and 6FDA, in which the absorption peaks at 7.1–8.3 ppm are assigned to the aromatic protons in polymer backbone. No absorption was detected in the range of >8.3 ppm, indicating that the concentration of amide group (–C(O)NH–) in polymer chains was lower than the detection limit of ^{1}H NMR (<5%). In other words, the polyimide possesses an imidization degree of >95%. Meanwhile, according to the data from Table 1, the resulting polyimides all got high yields (96–98%), and the inherent viscosities values of these polyimides were in the range of 0.40–0.71 dL/g, which indicated formation of high molar masses [26]. This was consistent with the fact that tough and flexible films could be obtained by coating and solvent evaporation of polymer solutions. However, the polyimide film based on APPT–PMDA (PI-4) was brittle because of the rigidity structure of the polymer chains. The elemental analysis data of the resulting polyimides also agreed well with the calculated values. The above results demonstrated that the diamine monomer APPT held a good polymerization activity to form soluble polyimides *via* one-step synthetic method.

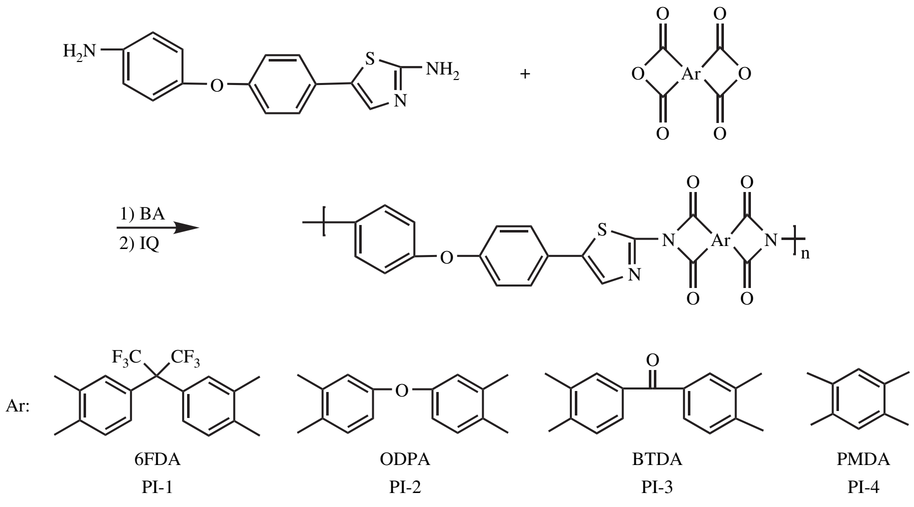

1) BA, benzoic acid; 2) IQ, isoquinoline.

Scheme 2. Synthesis of polyimides through one-step polymerization.

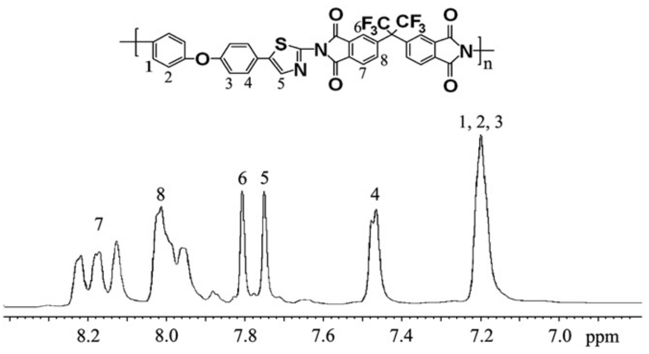

Fig. 4. ^{1}H NMR spectrum of polyimide based on APPT–6FDA (DMSO-d_6).

3.3. Solubility of the resulting polyimides

The solubilities of the resulting polyimides in several organic solvents at 3.0% are summarized in Table 2. The good solubility should be resulted from the flexible ether group, the noncoplanar factor and unsymmetrical structure in the polyimide main chain. The solubility varies depending upon the dianhydride used. PI-1 and PI-2 possesses the better solubility at room temperature, because of the presence of the trifluoromethyl and the flexible ether groups, respectively. As expected, PI-4 has poorer solubility, which was possible due to the rigidity structure of the polymer chains. It can be seen that the good solubility of PI-1 and PI-2 in THF indicate their potential applications in areas where temperature is sensitive.

3.4. X-ray diffraction of the polyimides

The crystallinity of the polyimides was examined by wide-angle X-ray diffraction analysis with graphite monochromatized CuKα radiation, 2θ ranging from 0° to 80°, using the polyimide powder obtained as samples. The results were shown in Fig. 5. The X-ray diffraction curves of these polyimides showed a set of wider diffraction peaks, these should be the evidences that indicated the polyimides holding heterogeneous morphology, and should also be a reason that could obtain transparent films from these polyimides. The X-ray diffraction curves of the polyimides based on APPT–BTDA and APPT–PMDA exhibited peaks around 20° and 26°, which indicated a little of crystalline morphologies in the resulting polyimide. This should be related to rigidity structure of the polymer chains. PIs based on APPT–6FDA and APPT–ODPA showed amorphous phase, and this is because of the presence of flexible group induces looser chain packing and reveals a large decrease in crystallinity. Therefore, the amorphous nature of the resulting polyimides would endow them a good solubility.

Table 2
Solubility data of the polyimides

Polymer	Solvent[a]					
	NMP	DMAc	DMF	DMSO	*m*-Cresol	THF
PI-1	++	++	++	++	++	++
PI-2	++	++	+	+	++	+
PI-3	++	+	+	+	+	−−
PI-4	+	+−	+−	+	+	−−

Qualitative solubility was determined at 3.0%(w/v); ++, soluble at room temperature; +, soluble on heating; +−, partially soluble; and −−, insoluble even on heating.

[a] NMP, *N*-methyl-2-pyrrolidone; DMAc, *N*,*N*-dimethylacetamide; DMF, *N*,*N*-dimethylformamide; DMSO, dimethyl sulfoxide.

3.5. Mechanical, electrical properties and water uptake

All of the polyimides could be processed into clear, flexible, and tough films, except the polyimide based on APPT–PMDA (PI-4) because of the rigidity structure of the polymer chains. These films were subjected to tensile tests. Table 4 shows the mechanical properties of the polyimides, including the tensile strength, tensile modulus as well as elongation at breakage. The polyimide films had tensile strength of 105.4–125.3 MPa, elongations at breakage of 6–13%, and tensile moduli of 2.19–2.48 GPa, which indicated strong and tough materials.

The dielectric constant values of the polyimides are presented in Table 3. In this study, all polyimide samples were prepared with the same curing process. Although the thicknesses of the polyimide films were different, the dielectric constants of the polyimide films thicker than 1 μm did not vary with the thickness [27,28]. Obviously, the dielectric

Table 1
Inherent viscosity and element analysis of polyimides

Polymer	Yield (%)	η_{inh}[a] (dL/g) (of PI)	Elemental analysis (%) of polyimides					
			Formula of PI (formula weight)		C	H	N	Film quality[b]
PI-1	98	0.63	$(C_{34}H_{15}N_3O_5F_6S)_n$ $(691.51)_n$	Calcd.	59.06	2.19	6.08	C, F & T
				Found	55.80	2.13	5.98	
PI-2	98	0.71	$(C_{31}H_{15}N_3O_6S)_n$ $(577.49)_n$	Calcd.	66.79	2.71	7.54	C, F & T
				Found	66.55	2.58	7.33	
PI-3	97	0.56	$(C_{32}H_{15}N_3O_6S)_n$ $(569.50)_n$	Calcd.	67.49	2.65	7.38	C, F & T
				Found	67.17	2.59	7.33	
PI-4	96	0.40	$(C_{25}H_{11}N_3O_5S)_n$ $(465.39)_n$	Calcd.	64.52	2.38	9.03	–
				Found	63.94	2.33	8.91	

[a] Inherent viscosity (η) determined on 0.5% solutions in a solvent (NMP) at 30 °C.

[b] C: clear; F: flexible; T: tough; –: brittle.

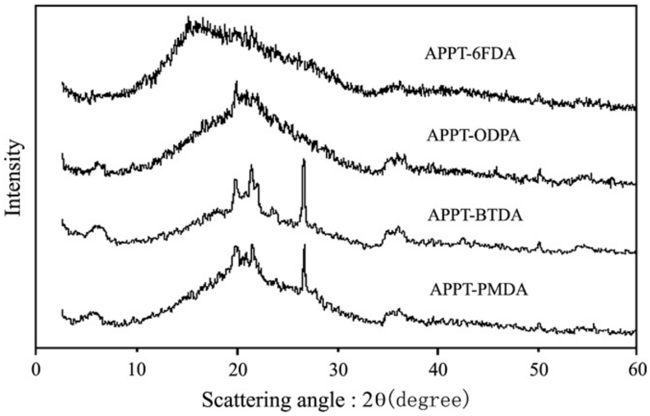

Fig. 5. Wide-angle X-ray diffraction curves of the polyimides.

constants for each sample were quite different, strongly depending on the chemical structure. It may be affected by decreasing the molecular packing efficiency of their chemical structures. A low molecular packing order can lead to a decrease in the number of polar group in unit volume. In other words, fewer polarizable groups in unit volume may lead to a lower dielectric constant for polyimide films [28].

Polyimides based on APPT had lower dielectric constants (3.01–3.18 at 10 MHz) compared with conventional polyimides such as PMDA–ODA polyimide film (3.44 at 10 MHz). The dielectric constant values were in increasing order for our samples: PI-1 < PI-2 < PI-3. PI-1 has the lowest dielectric constant owing to the presence of the bulky CF_3 groups. The bulky hexafluoroisopropylidene groups [$-C(CF_3)_2-$] in PI-1 could result in low molecular packing order from steric hindrance. In addition, the strong electronegativity of fluorine results in very low polarizability of the C–F bonds, reducing the dielectric constant. PI-2 has lower dielectric constant than PI-3 due to larger polarity of BTDA than ODPA. This could be explained by the existence of carbonyl groups in the PI-3 structure. The electron density of C atoms forms extra polarization by sliding on the oxygen atoms and this could cause an increase in the dipole number density. Because the responses of the electronic, atomic, and dipolar polarizable units vary with frequency, for each polyimide, the dielectric constants reduce gradually with the increment of the frequency. This behavior could be attributed to the dependence of the polarization mechanisms [29,30].

As water has a very high dielectric constant, absorption in even small amounts could affect the dielectric constant of polyimide films. Absorbed water in the package has a critical effect on the electrical properties of polyimide films [31]. Water uptake properties of the polyimide films were depicted in Table 3. The values were in the range of 0.30–0.44%, and in such order: PI-1 < PI-3 < PI-2. Because the hexafluoroisopropylidene group acts as a hydrophobic hindrance in the polyimide structure, PI-1 has the smallest value. Moreover, a structurally flexible polymer with bulky chemical groups in its structure shows more water uptake than a linear, rigid polymer [32]. So PI-2 shows higher water uptake values than PI-3 because of the more free volume between the molecules. As the results show in Table 3, the low water uptake and low dielectric constants of these polyimides present potential utility of the material in the microelectronics industry, where a low dielectric constant is desired to prevent crosstalk between conducting paths.

Table 3
Dielectric properties of polyimide films

Polymer	Thickness (μm)	Dielectric constant[a] (dry)				Water uptake (%)
		10 MHz	20 MHz	200 MHz	1 GHz	
PI-1	36	3.01	2.95	2.95	2.89	0.30
PI-2	38	3.13	3.06	3.06	2.96	0.44
PI-3	30	3.18	3.11	3.12	3.00	0.39
Kapton[b]	36	3.44	3.42	3.32	3.25	0.53

[a] Measured by Agilent 4291B at room temperature (dry dielectric constant).
[b] Polyimide derived from PMDA–ODA.

Table 4
Mechanical properties of the polyimides

Polymer	Tensile strength (MPa)	Tensile modulus (GPa)	Elongation at breakage (%)
PI-1	110.7	2.48	10
PI-2	125.3	2.42	13
PI-3	105.4	2.19	6

3.6. Thermal properties of the resulting polyimides

The thermal properties of the polyimides, which were evaluated by DSC and TGA methods, are listed in Table 5. DSC and TGA curves of the polyimides are shown in Figs. 6 and 7, respectively. DSC revealed rapid cooling from 400 °C to room temperature produced predominantly amorphous samples, so that the T_g of polymer could be easily read in the second-heating trace of DSC. The T_g values of these polyimides were in the range of 268.2–328.8 °C. In comparison with commercial polyimide, the T_g values of these polyimides are higher than commercial polyimide, Ultem 1000 (T_g, 217 °C), based on bisphenol-A diphthalic anhydride and *m*-phenylene diamine [33]. However, the T_g values of these polyimides are lower than Kapton films derived from PMDA–ODA (T_g, 390 °C) [33].

As we expected, the T_g values of these PIs depended on the structure of the dianhydride component, and decreased with increasing flexibility of the polyimides backbones based on

Table 5
Data of thermal analysis of the polyimides

Polymer	T_g[a] (°C)	In N_2[b] (°C)		In air[b] (°C)		Char yield[c] (%)
		T_5	T_{10}	T_5	T_{10}	
PI-1	268.2	452	487	422	457	54.18
PI-2	300.0	468	505	437	462	57.30
PI-3	320.2	489	523	439	482	59.31
PI-4	328.8	507	548	458	499	63.33

[a] T_g measured by DSC at a scanning rate of 10 °C/min in flowing nitrogen.
[b] Temperature at a 5 or 10% weight loss at a 20 °C/min heating rate.
[c] Residual weight (%) at 800 °C in nitrogen.

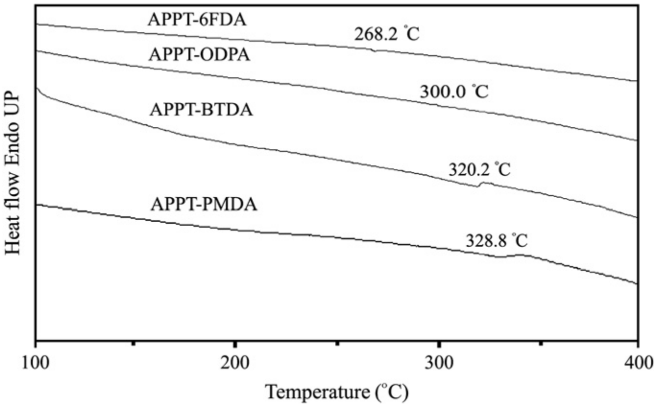

Fig. 6. DSC thermograms of PIs at heating rate of 20 °C/min in nitrogen.

applied structure of dianhydride. PI-1 showed a lower T_g because of the presence of the bulky CF_3 groups between the phthalimide units. PI-4 exhibited the highest T_g due to the rigid pyromellitimide unit. Clearly, the difference in T_g's was attributed to the rigidity and packing of the polymer chains. According to Fig. 5, some of the resulting polyimides should exhibit melting peaks from the crystalline morphology in DSC curves. However, no melting peaks were observed in the DSC curves presented in Fig. 6, the T_m values represented the crystalline morphology was not obtained from the DSC curves certainly. These probably were that the T_m values of the resulting polyimides were too high to have overstepped measure range of used DSC meter [34,35].

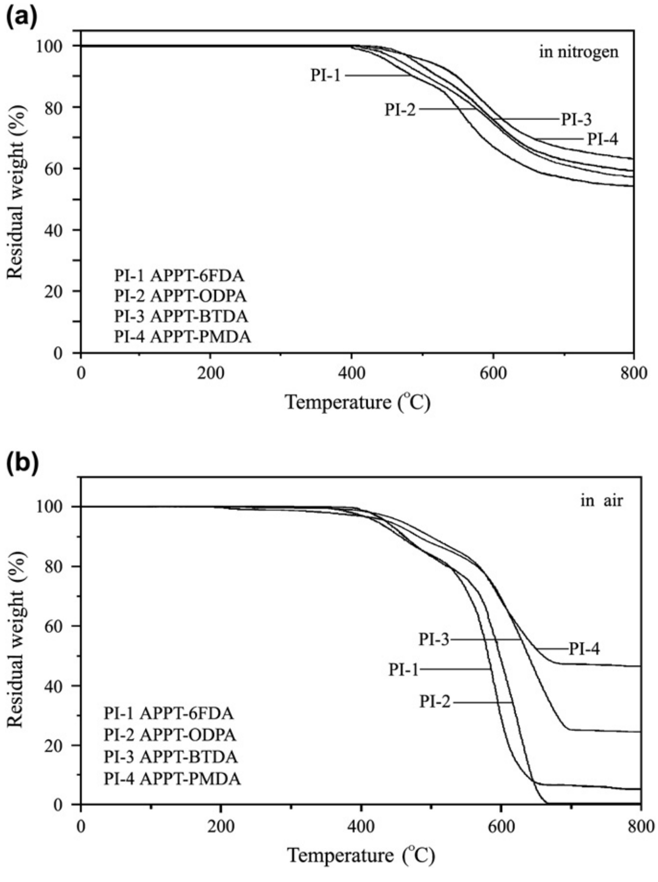

Fig. 7. TGA curves of PIs at a heating rate of 20 °C/min (a) in N_2 and (b) in air.

For the thermal stability of the polyimides, Table 5 gave the temperature of the 5% and 10% gravimetric loss in nitrogen and in air, respectively, i.e. T_5 and T_{10} values. T_5 and T_{10} of the polyimides reached 452–507 °C and 487–548 °C in nitrogen, while those of them were in the range 422–458 °C and 457–499 °C in air, and the amount of residue of all polyimides at 800 °C in nitrogen atmosphere was higher than 54.18%, especially, PI-4 had highest yield up to 63.33%. Obviously, the data from thermal analysis showed that the resulting polyimides had fairly high thermal stability and the thermooxidative stability derived from thiazole rings.

4. Conclusion

A novel kind of unsymmetrical diamine with thiazole ring, i.e. 2-amino-5-[4-(4′-aminophenoxy)phenyl]-thiazole (APPT), was successfully synthesized in high purity and high yields in this work, and the resulting APPT was employed to react with various aromatic dianhydrides by one-step polyimidation process. The experimental results indicate that the novel polyimides obtained have high T_g values, excellent thermal and thermooxidative stability, as well as good solubility in organic solvents. These polymers also have good mechanical properties with low dielectric constants. These features are desirable for polyimides as potential candidate for microelectronics packaging applications.

Acknowledgments

We thank the financial support from the Opening Foundation of State Key Laboratory of Applied Organic Chemistry.

References

[1] Wilson D, Stenzenberger HD, Hergenrother PM, editors. Polyimides. New York: Chapman and Hall; 1990. p. 58–77.
[2] Ghosh MK, Mittal KL, editors. Polyimides fundamentals and applications. New York: Marcel Decker; 1996. p. 7–48.
[3] Yang CP, Su YY. Polymer 2005;46:5797.
[4] Zhang SJ, Li YF, Wang XL, Zhao X, Shao Y, Yin DX, et al. Polymer 2005;46:11986.
[5] Wang XL, Li YF, Zhang SJ, Ma T, Shao Y, Zhao X. Eur Polym J 2006;42:1229.
[6] Ahn SK, Kim HS, Kim YH, Kwon SK. Macromolecules 2003;36:2327.
[7] Shao Y, Li YF, Zhao X, Wang XL, Ma T, Yang FC. J Polym Sci Part A Polym Chem 2006;44:6836.
[8] Takekoshi T, Kochanowski JE, Manello JS, Webber MJ. J Polym Sci Part A Polym Chem Ed 1985;23:1759.
[9] Takekoshi T, Kochanowski JE, Manello JS, Webber MJ. J Polym Sci Polym Symp 1986;74:93.
[10] Takekoshi T. Polymer 1987;19:191.
[11] Seymour RB, Krishenbaum GS, editors. High performance polymers: their origin and development. Amsterdam: Elesvier; 1986. p. 195–205.
[12] Aihara Y, Cebe P. Polym Eng Sci 1994;34(16):1275.
[13] Fang XZ, Wang Z, Yang ZH, Gao LX, Ding MX. Polymer 2003;44:2641.
[14] Xu JW, Chng ML, Chung TS, He CB, Wang R. Polymer 2003;44:4715.

[15] Yang CP, Su YY. Polymer 2003;44:6311.

[16] Fang XZ, Yang ZH, Zhang SB, Gao LX, Ding MX. Polymer 2004;45:2539.

[17] Yang CP, Su YY, Wu KL. J Polym Sci Part A Polym Chem 2004;42:5424.

[18] Zhang M, Wang Z, Gao LX, Ding MX. J Polym Sci Part A Polym Chem 2006;44:959.

[19] In I, Kim SY. Polymer 2006;47:547.

[20] Liu S, Sun W, He BJ, Shen ZQ. Eur Polym J 2004;40:2043.

[21] Leng WN, Zhou YM, Xu QH, Liu JZ. Polymer 2001;42:9253.

[22] Al-Dujaili Amar H, Atto Amir T, Al-Kurde Adel M. Eur Polym J 2001;37:927.

[23] Sek D, Wanic A, Schab-Balcerzak E. J Polym Sci Part A Polym Chem 1995;33:547.

[24] Mehdipour-Ataei S, Arabi H, Bahri-Laleh N. Eur Polym J 2006;42:2343.

[25] Sek D, Pijet P, Wanic A. Polymer 1992;33:190.

[26] Chen H, Yin J. J Polym Sci Part A Polym Chem 2003;41:2026.

[27] Liang T, Makita Y, Kimura S. Polymer 2001;42:4867.

[28] Deligoz H, Yalcinyuva T, Ozgumus S, Yildirim S. J Appl Polym Sci 2006;100:810.

[29] Muruganand S, Narayandasss SaK, Mangalaraj D, Vijayan TM. Polym Int 2001;50:1089.

[30] Alegaonkar RS, Mandela AB, Sainker SR, Bhoraskar VN. Nucl Instr Methods Phys Res B 2002;194:281.

[31] Maier G. Prog Polym Sci 2001;26:3.

[32] Lee C, Shu Y, Han H. J Polym Sci Part B Polym Phys 2002;40:2190.

[33] Takekoshi T, editor. Kirk–Othmer encyclopedia of chemical technology. 4th ed., vol. 19. New York: John Wiley & Sons; 1996. p. 813–37.

[34] Ratta V, Ayamben A, McGrath JE, Wilkes GL. Polymer 2001;42:6173.

[35] Liu XQ, Yamanaka K, Mitsutoshi JK, Kakimoto MA. Chem Mater 2000;12:3885.